Hindawi Publishing Corporation
International Journal of Photoenergy
Volume 2015, Article ID 760376, 6 pages
http://dx.doi.org/10.1155/2015/760376

Research Article

Optical Properties of Indium Doeped ZnO Nanowires

Tsung-Shine Ko,[1] Sin-Liang Ou,[2] Kuo-Sheng Kao,[3] Tz-Min Yang,[2] and Der-Yuh Lin[1]

[1]*Department of Electronic Engineering, National Changhua University of Education, No. 1, Jin-De Road, Changhua 500, Taiwan*
[2]*Department of Materials Science and Engineering, National Chung Hsing University, Taichung 40227, Taiwan*
[3]*Department of Computer and Communication, SHU-TE University, Kaohsiung 824, Taiwan*

Correspondence should be addressed to Der-Yuh Lin; dylin@cc.ncue.edu.tw

Received 17 December 2014; Revised 9 February 2015; Accepted 10 February 2015

Academic Editor: Shyh-Jer Huang

We report the synthesis of the ZnO nanowires (NWs) with different indium concentrations by using the thermal evaporation method. The gold nanoparticles were used as the catalyst and were dispersed on the silicon wafer to facilitate the growth of the ZnO NWs. High resolution transmission electron microscopy confirms that the ZnO NWs growth relied on vapor-liquid-solid mechanism and energy dispersion spectrum detects the atomic percentages of indium in ZnO NWs. Scanning electron microscopy shows that the diameters of pure ZnO NWs range from 20 to 30 nm and the diameters of ZnO:In were increased to 50–80 nm with increasing indium doping level. X-ray diffraction results point out that the crystal quality of the ZnO NWs was worse with doping higher indium concentration. Photoluminescence (PL) study of the ZnO NWs exhibited main photoemission at 380 nm due to the recombination of excitons in near-band-edge (NBE). In addition, PL results also indicate the slightly blue shift and PL intensity decreasing of NBE emission from the ZnO NWs with higher indium concentrations could be attributed to more donor-induced trap center generations.

1. Introduction

Zinc oxide (ZnO) is one of the most favorable materials for blue/UV-associated optoelectronic devices and exciton-related device applications due to a wide band gap (3.37 eV) at room temperature and a large excitonic binding energy (60 meV) in comparison with GaN (28 meV) [1]. In recent, one-dimensional semiconductors have attracted much attention for nanoscale optoelectronic devices such as field effect transistors (FETs) [2, 3], gas sensors [4, 5], lasers [6], and photovoltaic applications [7]. In general, doping in wide band gap semiconductors often causes dramatic changes in the electric and optical properties. The conduction of transparent ZnO films could increase with cationic doping of group III elements, such as B, Al, Ga, and In. [8]. Among these ZnO with different dopants, In-doped ZnO films show similar electrical conductivity and better transparency in both the visible and IR regions compared to indium tin oxide. Thus, ZnO:In can be widely used as transparent conductors in optoelectronic applications [9, 10]. ZnO exhibits n-type semiconducting behavior due to native defects including Zn interstitials, oxygen vacancies, or hydrogen interstitials. This makes it difficult to understand the main effect of additional dopants in terms of the structure and optoelectric properties of ZnO. Typically, ZnO doped with indium (>1%) wire-like (wires, belts, and rods) nanostructures were synthesized by thermal evaporation [11] and sol-gel [12] methods, recently. Despite many literatures having revealed main material properties of ZnO, however, the reports related to ZnO wire-like nanostructures with low indium doping concentration are still few and limited. In this paper, we successfully synthesized ZnO:In nanowires (NWs) with different indium doping concentration for comparison using gold nanoparticles as catalyst coated on Si substrates. The influence of the indium concentration on structural and optical properties of ZnO and ZnO:In NWs were investigated by scanning electron microscopy (SEM), transmission electron microscopy (TEM), X-ray diffraction (XRD), energy dispersive spectrometry (EDS), selected area electron diffraction (SAED), and photoluminescence (PL). A series of experiments revealed not only growth mechanism but also analyzed main exciton behavior for the ZnO NWs with different indium doping concentrations.

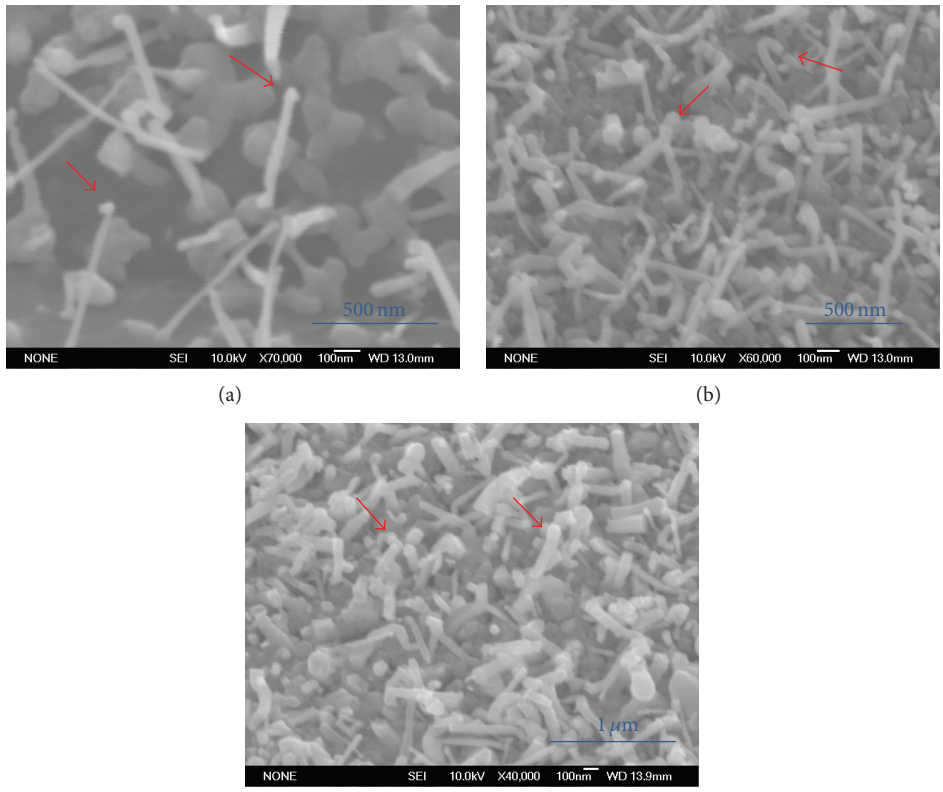

Figure 1: SEM images of ZnO:In NWs with different indium concentrations (a) undoped, (b) 0.86%, and (c) 0.95%. The red arrows point out the nanoparticles.

2. Experiments

P-type (001) oriented silicon wafers were prepared as substrates. Gold nanoparticles were produced by chemical reduction of gold tetrahydrate ($HAuCl_4$) with sodium citrate and then spread onto a native oxide coated silicon wafer with a self-assembled monolayer of 3-aminopropyltrimethoxysilane as adhesion layer. The width and density of gold nanoparticles are 10–20 nm and $6 \times 10^8\,\text{cm}^{-2}$ examined by scanning electron microscopy (SEM) images. A two-zone vacuum furnace was used for the growth of ZnO and ZnO:In NWs. 1.350 g zinc balls mixed with 0, 0.120, and 0.240 g indium balls, respectively, were positioned upstream in the vacuum furnace for providing vapor sources, while the substrates were placed downstream for the condensation of materials. Oxygen flowed through the system with a flow rate of 150 sccm used as reactive gas. During the growth, the temperatures elevated to 1050°C for sources and 700°C for sample, and the system pressure was kept at about 0.1 torr. SEM (JEOL, JSM 6500F) and TEM (JEOL, JEM 2010G, operating at 200 kV) were measured to investigate the morphologies and microstructures of the samples. For the TEM investigation, the samples should be further treated. We put the samples into a methanol solution and then performed the ultrasonic treatment. After this process for 1-2 minutes, the ZnO NWs were separated from the substrate. Subsequently, a drop of the suspension on a holey carbon film supported by a 3-mm-diameter copper mesh was dried in air. Finally, the sample can be fixed at the TEM holder for microstructural observation. The crystal structure and phase purity were characterized by XRD measurements with Cu Kα as the radiation source and SAED patterns affiliated to the TEM. The chemical compositions were examined by EDS attached to the TEM. PL spectra were performed at room temperature by using TRIAX-320 spectrometer equipped with a 25 mW He-Cd laser with the wavelength of 325 nm.

3. Results and Discussion

The morphologies and microstructures of the as-grown materials were characterized and analyzed by SEM. Figure 1 shows the SEM images of the ZnO (a) and ZnO:In (b) (c) NWs deposited on the gold nanoparticles coated Si substrates. The diameters of pure ZnO NWs range from 20 to 30 nm and the diameters of ZnO:In with different indium doping level were in the range of 20–50 and 20–80 nm, respectively. Also, the lengths of all the ZnO and ZnO:In were about several hundred nanometers. Apparently the incorporation of indium could influence the diameter of ZnO:In NWs. Except the wire-like structure observed from SEM, some unknown nanoparticles could be found on the top of NWs which are pointed out by red arrowheads in Figures 1(a)–1(c), suggesting that they act as catalyst in the growth process of

NWs. This feature could be further confirmed by using TEM and EDS measurements.

XRD diffraction patterns in theta-2theta geometry have been measured for examining the crystal quality and phase purity of the as-deposited materials which is shown in Figure 2. No diffraction peaks of indium or other impurities phases were revealed in any of our samples from XRD results. All the diffraction peaks in XRD spectra are corresponding to the ZnO crystal faces and the intensity of the (002) peak is much stronger than other ZnO peaks in the three of our samples, indicating the (002) crystal face might be the primary face of the NWs and the doping with small amount of indium did not affect the (002) orientation. The intensity and full-width half-maximum (FWHM) of the diffraction peaks, measures of crystal quality, in XRD patterns decreases and increases as the function of indium content, respectively. The degradation in crystal quality may be interpreted as the local disorder and lattice distortion due to the substitution of a zinc atom by an indium atom.

TEM, SAED, and EDS measurements were carried out to obtain more detailed structure and composition characterization of the individual NW. It was found that well NW structures with diameter of about 30 nm and a nanoparticle capped at its top in our TEM observations shown in Figures 3(a), 3(b), and 3(c). The SAED patterns of these three samples were also exhibited in Figures 3(a), 3(b), and 3(c). The planes of some diffraction dots were analyzed and marked; meanwhile, the zone axes of these samples were all identified to [001]. The EDS analysis indicates that the nanoparticles consisted mainly of gold and a small quantity of zinc, indium, and oxygen elements, while the stem of the NWs composed of only zinc, indium, and oxygen. The representative EDS spectra of the stem and tip part from ZnO:In NWs are shown in Figures 4(a) and 4(b). Through the measurement of EDS, the atomic percentages of indium were detected to be 0, 0.86, and 0.95 at. % in ZnO NWs for samples prepared with 0, 0.120, and 0.240 g indium. Since the vapor pressure is about 8×10^{-2} atm for Zn and 7×10^{-8} atm for In at 700°C in sample area, the huge difference of Zn/In mole ratio between the sources and the products in our experiment may be owing to a large discrepancy of vapor pressure between the two elements [13]. The vapor-liquid-solid (VLS) growth mechanism which was first proposed by Wanger and Ellis [14] for the growth of silicon whisker has been wildly used in the synthesis of wire-like nanostructures, such as Si, GaN, ZnO, and In_2O_3 recently. According to the VLS process, two significant characteristics of the nanostructures will be mentioned. First, the presence of metal particles located at the growth fronts is demanded, which act as catalytic sites. Second, the dimension of the nanostructure is usually determined by the size of metal particle since the longitudinal growths of nanostructures only take place on the interface of metal particle. Both two features are in agreement with our results obtained from SEM and TEM images, which were considered as the evidence for the growth of VLS mechanism. In addition, the size of gold nanoparticles, before and after the growth of NWs, became larger which may result from the formation of Au-In-Zn alloy examined by EDS results during the period of growth. The

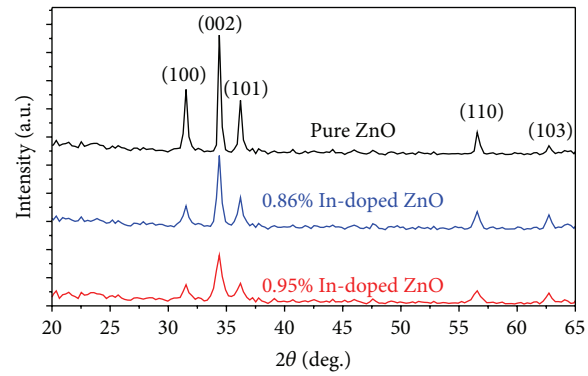

Figure 2: XRD patterns of ZnO and ZnO:In NWs.

SAED patterns which revealed the ZnO and ZnO:In NWs are single crystalline which are shown in insets to Figures 3(a), 3(b), and 3(c).

PL is a nondestructive and sensitive technique for investigating the band structure and defect levels of semiconductors. Figure 5 shows the PL spectra recorded at room temperature, using 325 nm line of 25 mW He-Cd laser for the excitation of ZnO and ZnO:In NWs. At the UV region in PL spectra, three strong near-band-edge (NBE) emissions associated with the exciton centered at about 380 nm were found, and on the other hand three weak broad defect-related green band (GB) emissions centered at around 540 nm were also observed at the visible light region. While we focus on the NBE emission (inset in Figure 5), the peak position and PL intensity shifts slightly to higher energy (blue-shift) and depresses with the increasing doping level of indium, respectively. The phenomenon of blue-shift can be attributed to the widening of the optical band-gap due to Burstein-Moss effect [15] which is interpreted that at high electron concentrations, due to small density of states of ZnO near the conduction band minimum, the conduction band edge is filled with excessive carriers donated by donor indium, coming from the substitution of indium for zinc and results in a blue-shift of optical transitions. Afterwards, when ZnO:In samples are excited, the excited electrons will be taken up higher energy levels and lead to a blue-shift of radiative recombination. Similar results were reported by Chen et al. in ZnO:In NWs by sol-gel method [16]. Kim and Park measured the variation of band-gap as the function of carrier concentration [17]. The NBE peak poison blue-shifted, comparing to the pure ZnO, about 25 and 43 meV for ZnO doped with indium 0.86 and 0.95 at. %, respectively. According to Kim and Park's research, we suppose the carrier concentration of In-doped ZnO NWs (0.95%) would be in the region of 1.1×10^{19} cm^{-3}. Furthermore, the depression of the NBE emission intensity can be explained by the formation of donor-induced nonradiative recombination centers originating from the incorporation of indium [18]. In comparison to higher In concentration than 1%, Bae et al. proposed that NBE emission of ZnO:In nanowires with 10~20% indium concentration shift to the lower energy region [19]. They suggested the high doping effect causes the decrease of band

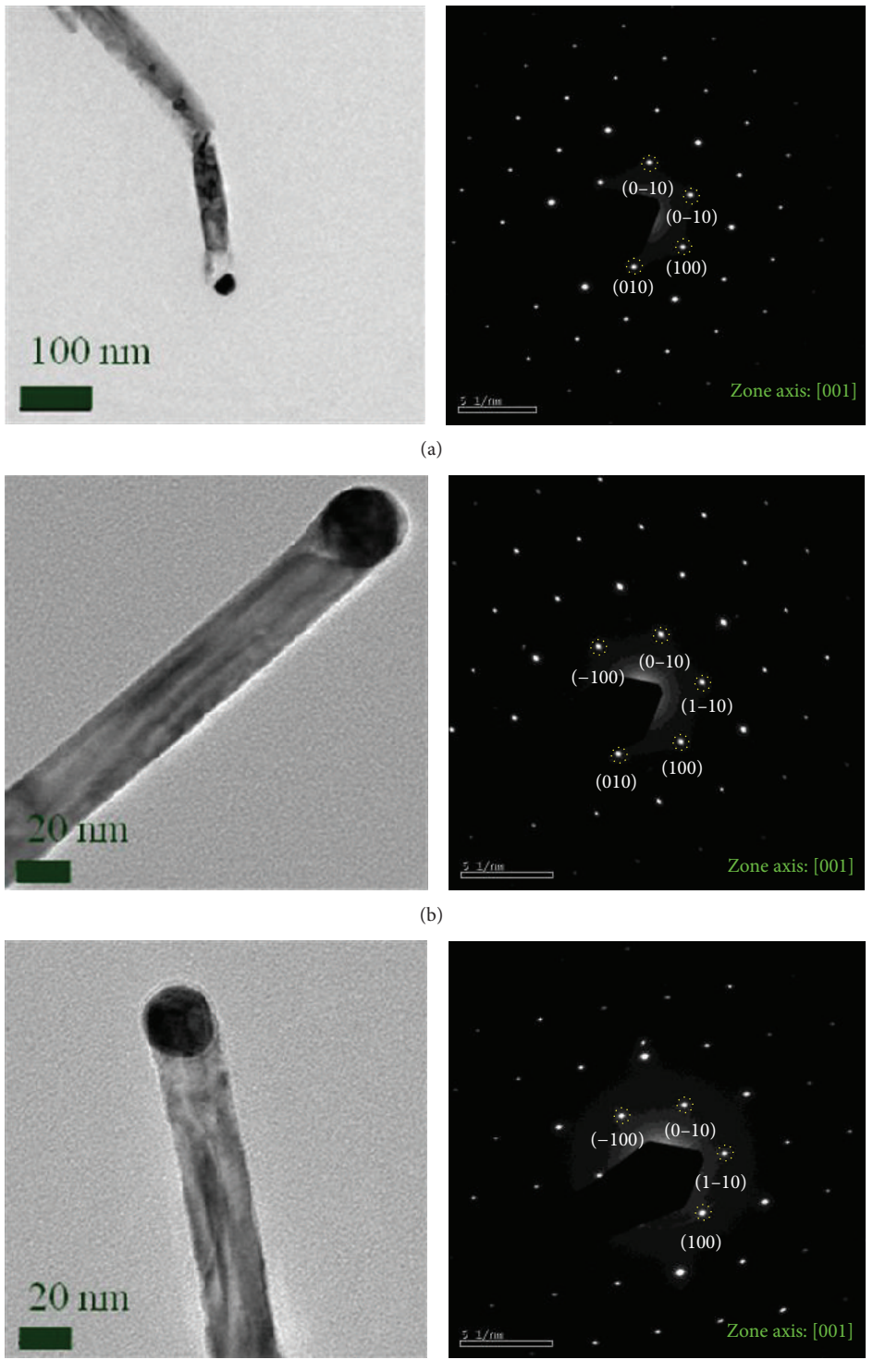

Figure 3: TEM images and the corresponding SAED patterns of ZnO:In NWs with different indium concentrations (a) undoped, (b) 0.86%, and (c) 0.95%.

gap and the energy broadening of valence band states. As the doped elements enter the ZnO crystal lattices, the additional localized band edge states form at the doped sites, with a reduction of band gap. After that, it is well known that the incomplete oxidation of oxide compound semiconductors will lead to the production of nonstoichiometric defects: oxygen vacancies (V_o), and the GB emission is suggested to be the radiative recombination of electrons in singly occupied oxygen vacancies (V_o^+) with photoexcited holes in the valence band [20]. The PL spectrum of pure ZnO NWs

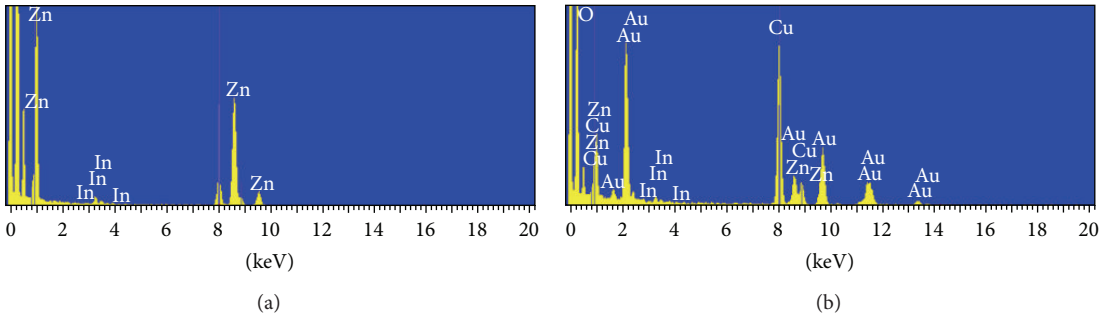

FIGURE 4: The representative EDS spectra results of (a) the stem and (b) tip part from ZnO:In NWs.

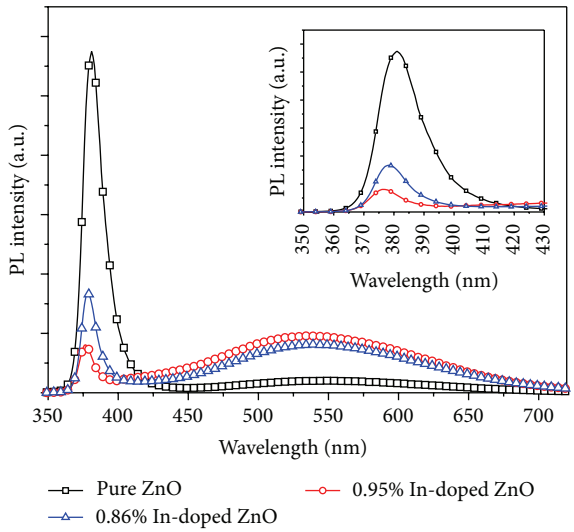

FIGURE 5: Room temperature PL spectra of ZnO and ZnO:In NWs. The inset shows the UV-region PL spectra.

exhibited a GB emission with an extremely low intensity verified ZnO NWs possessed of low oxygen vacancies were synthesized. Moreover, the intensities of GB emission from ZnO:In nanowires were slightly enhanced, which may be ascribed to the incorporation of indium.

4. Conclusion

In conclusion, we have synthesized ZnO NWs with different indium doping concentrations on gold nanoparticles coated Si substrates in the vacuum furnace by suing a thermal evaporation method. From SEM investigations, the diameter range of NWs increases after the incorporation of indium. XRD shows a preferred (002) crystal face without any other impurity phase in all of our samples and the crystal quality of NWs degrades with the increasing of indium concentration. The VLS mechanism may be dominant in the growth of ZnO NWs examined by SEM and TEM images. The NBE emission peak showing a slight blue-shift with the increasing indium doping level could be attributed to Burstein-Moss effect. With the incorporation of indium, the NBE emission intensity depresses. The defect-related GB emission intensity is slightly enhanced after the doping of indium as well. According to the structural and optical properties of lightly indium doped ZnO, it would be beneficial for electrooptical applications.

Conflict of Interests

The authors declare that there is no conflict of interests regarding the publication of this paper.

Acknowledgment

This study was supported by the National Science Council of Taiwan, under Contract NSC 102-2218-E-018-003.

References

[1] X. W. Sun and H. S. Kwok, "Optical properties of epitaxially grown zinc oxide films on sapphire by pulsed laser deposition," *Journal of Applied Physics*, vol. 86, p. 408, 1999.

[2] H. Kind, H. Yan, B. Messer, M. Law, and P. Yang, "Nanowire ultraviolet photodetectors and optical switches," *Advanced Materials*, vol. 14, no. 2, pp. 158–160, 2002.

[3] M. S. Arnold, P. Avouris, Z. W. Pan, and Z. L. Wang, "Field-effect transistors based on single semiconducting oxide nanobelts," *The Journal of Physical Chemistry B*, vol. 107, no. 3, pp. 659–663, 2003.

[4] Z. L. Wang, "Functional oxide nanobelts: materials, properties and potential applications in nanosystems and biotechnology," *Annual Review of Physical Chemistry*, vol. 55, pp. 159–196, 2004.

[5] W. Q. Peng, S. C. Qu, G. W. Cong, and Z. G. Wang, "Synthesis and temperature-dependent near-band-edge emission of chain-like Mg-doped ZnO nanoparticles," *Applied Physics Letters*, vol. 88, no. 10, Article ID 101902, 2006.

[6] J. C. Johnson, K. P. Knutsen, H. Yan et al., "Ultrafast carrier dynamics in single ZnO nanowire and nanoribbon lasers," *Nano Letters*, vol. 4, no. 2, pp. 197–204, 2004.

[7] P. S. Venkatesh, V. Ramakrishnan, and K. Jeganathan, "Vertically aligned indium doped zinc oxide nanorods for the application of nanostructured anodes by radio frequency magnetron sputtering," *CrystEngComm*, vol. 14, no. 11, pp. 3907–3914, 2012.

[8] T. Minami, H. Sonohara, T. Kakumu, and S. Takata, "Highly transparent and conductive $Zn_2In_2O_5$ thin films prepared by RF magnetron sputtering," *Japanese Journal of Applied Physics*, vol. 34, no. 8, p. L971, 1995.

[9] A. C. Wang, J. Dai, J. Z. Cheng et al., "Charge transport, optical transparency, microstructure, and processing relationships in

transparent conductive indium-zinc oxide films grown by low-pressure metal-organic chemical vapor deposition," *Applied Physics Letters*, vol. 73, no. 3, pp. 327–329, 1998.

[10] L. P. Peng, L. Fang, X. F. Yang et al., "Effect of annealing temperature on the structure and optical properties of In-doped ZnO thin films," *Journal of Alloys and Compounds*, vol. 484, no. 1, pp. 575–579, 2009.

[11] J. Jie, G. Wang, X. Hang et al., "Indium-doped zinc oxide nanobelts," *Chemical Physics Letters*, vol. 387, no. 4–6, pp. 466–470, 2004.

[12] D. Vorkapic and T. Matsoukas, "Effect of temperature and alcohols in the preparation of titania nanoparticles from alkoxides," *Journal of the American Ceramic Society*, vol. 81, no. 11, pp. 2815–2820, 1998.

[13] http://www.powerstream.com/vapor-pressure.htm.

[14] R. S. Wanger and W. C. Ellis, "Vapor-liquid-solid mechanism of single crystal growth," *Applied Physics Letters*, vol. 4, p. 89, 1964.

[15] E. Burstein, "Anomalous optical absorption limit in InSb," *Physical Review*, vol. 93, no. 3, pp. 632–633, 1954.

[16] Y. W. Chen, Y. C. Liu, S. X. Lu et al., "Optical properties of ZnO and ZnO:In nanorods assembled by sol-gel method," *The Journal of Chemical Physics*, vol. 123, no. 13, Article ID 134701, 2005.

[17] K. J. Kim and Y. R. Park, "Large and abrupt optical band gap variation in In-doped ZnO," *Applied Physics Letters*, vol. 78, no. 4, article 475, 2001.

[18] Y. Cao, L. Miao, S. Tanemura et al., "Optical properties of indium-doped ZnO films," *Japanese Journal of Applied Physics, Part 1: Regular Papers and Short Notes and Review Papers*, vol. 45, no. 3A, pp. 1623–1628, 2006.

[19] S. Y. Bae, C. W. Na, J. H. Kang, and J. Park, "Comparative structure and optical properties of Ga-, In-, and Sn-doped ZnO nanowires synthesized via thermal evaporation," *The Journal of Physical Chemistry B*, vol. 109, no. 7, pp. 2526–2531, 2005.

[20] K. Vanheusden, W. L. Warren, C. H. Seager, D. R. Tallant, J. A. Voigt, and B. E. Gnade, "Mechanisms behind green photoluminescence in ZnO phosphor powders," *Journal of Applied Physics*, vol. 79, no. 10, pp. 7983–7990, 1996.